Complicated Double-Orifice Mitral Regurgitation: Combined Hemodynamic Assessment Using Echocardiography and Four-Dimensional Flow Magnetic Resonance Imaging

Jeesoo Lee, PhD, Nadia El Hangouche, MD, Aakash N. Gupta, BS, Michael Markl, PhD, Susan Kim, MD, Jane Wilcox, MD, MSc, and James D. Thomas, MD, FASE, *Chicago and Evanston, Illinois*

INTRODUCTION

A 57-year-old woman was referred to our hospital for surgical repair of her mitral valve. She was diagnosed with mitral valve prolapse at the age of 18. Three years previous to this presentation, she was asymptomatic and able to run 10 to 15 miles at an 8-min pace. She now reported being able to run only 1 mile at a 10-min pace but otherwise denied symptoms. She had a family history of sudden cardiac death (both father and mother) and a personal history of several syncopal episodes with palpitations, most recently 3 years earlier. Twelve-lead electrocardiography (Figure 1) demonstrated a prolonged corrected QT interval (497 msec) but was otherwise unremarkable.

CASE PRESENTATION

Transthoracic echocardiography demonstrated significant bileaflet mitral valve prolapse with mitral annular disjunction (Figure 2A, Video 1) and a Pickelhaube sign[1,2] (sudden apical myocardial movement in late systole; Figure 2B). An apical two-chamber (Figure 3A, Video 2) and a short-axis color Doppler echocardiogram (Figure 3B, Video 3) demonstrated two distinct centrally directed late systolic regurgitant flow jets on either side of the A2-P2 leaflet, near the posteromedial (A3-P3) and anterolateral (A1-P1) commissures. The effective regurgitant orifice area (EROA) was measured for each orifice using the standard proximal isovelocity surface area method,[3] resulting in a total area of about 0.36 cm^2, which falls into the range of moderately severe mitral regurgitation (MR) according to 2017 American Society of Echocardiography guidelines.[4] However, both proximal convergence zones arose near the commissures, with adjacent ventricular walls limiting the flow convergence zone to a spreading angle of about 120° rather than full hemisphere (i.e., 180°; Figure 4, Video 4). As a result, EROA was reduced to about 0.24 cm^2.[5] When the nonholosystolic nature appreciated by continuous-wave Doppler measurement was factored into the calculation, the regurgitant volume (Rvol) was 30 mL, with a regurgitant fraction of 35%, reducing the severity to mild to moderate MR.[4] Additionally, volumetric quantification was performed. Biplane left ventricular (LV) stroke volume was 86 mL, while stroke volume in the LV outflow tract was 65 mL, yielding an Rvol estimated at 21 mL. Using mitral inflow instead of LV stroke volume predicted a much larger Rvol of 60 mL, reflecting overestimation of inflow due to annular dilation. All volumetric measurements related to the left ventricle and MR are listed in Table 1. Other parameters of regurgitant severity were less helpful because of the multiple jets and nonholosystolic flow, with the total area of both jets exceeding 50% of left atrial area and the summed vena contracta areas from three-dimensional (3D) imaging adding to 0.77 cm^2, reflective of poor lateral resolution of 3D color Doppler imaging.

To better assess the functional significance of the MR, the patient underwent exercise echocardiography and performed at high functional capacity (17 METs and 14 min on the Bruce protocol), with no significant increase in MR severity. However, of concern was the development of bigeminy early in exercise, resolving at peak but followed by multiple short runs (four or five beats) of polymorphic ventricular tachycardia (PMVT) approaching 300 beats/min, beginning about 90 sec after exercise and lasting about 1 min before reverting to bigeminy and then occasional premature ventricular complexes (Figure 5).

Because of complicated MR, PMVT, and bileaflet mitral valve prolapse, cardiac magnetic resonance imaging (CMR) was performed with T1 mapping of pre- and postcontrast images to assess fibrosis as a potential nidus for arrhythmia. Mitral annular disjunction was also observed (Figure 2C, Video 5). Mild LV enlargement (97 mL/m^2) with a mildly reduced ejection fraction of 47% was noted. No definite late gadolinium enhancement was seen, and extracellular volume was normal. Rvol of 20 mL was calculated using the volumetric method, subtracting aortic forward flow volume from LV stroke volume.

At the end of the standard CMR protocol, time-resolved 3D phase-contrast magnetic resonance imaging (MRI) with three-directional velocity encoding (four-dimensional [4D] flow MRI[6]) was performed to elucidate the flow and measure Rvol directly at the valve in addition to the conventional CMR volumetric method.[4] Four-dimensional flow

From the Department of Radiology, Northwestern University, Feinberg School of Medicine (J.L., A.N.G., M.M.), the Department of Cardiology, Northwestern Memorial Hospital (J.L., N.E.H., S.K., J.W., J.D.T.), Chicago, and the Department of Biomedical Engineering, Northwestern University, McCormick School of Engineering, Evanston (M.M.), Illinois.

Keywords: Bileaflet mitral valve prolapse, Mitral regurgitation, Double orifice, Nonholosystolic, 4D flow MRI

This work was supported by grants from the Irene D. Pritzker Foundation, GE Ultrasound, and Abbott Vascular.

Conflicts of interest: Dr. Thomas has received consulting fees and research support from GE Medical, Abbott Vascular, Edwards Lifesciences, and Caption Health, and his wife is employed by Caption Health.

2468-6441

https://doi.org/10.1016/j.case.2020.08.001

VIDEO HIGHLIGHTS

Video 1: Mitral valve prolapse with mitral annular disjunction (MAD) illustrated by transthoracic echocardiography.
Video 2: Apical two-chamber color Doppler echocardiogram showing two distinct centrally directed late systolic regurgitant flow jets.
Video 3: Short-axis color Doppler echocardiogram showing two distinct jets occurring at A1-P1 and A3-P3.
Video 4: Flow convergence zone restricted by the nearby LV wall.
Video 5: Apical three-chamber cine MRI showing bileaflet mitral valve prolapse.
Video 6: Apical two-chamber cross-sectional 4D flow MRI velocity magnitude image showing two distinct centrally directed flow jets.
Video 7: Short-axis cross-sectional 4D flow MRI velocity magnitude image showing two distinct jets occurring at A1-P1 and A3-P3.
Video 8: Three-dimensional flow path lines in left heart constructed with 4D flow MRI velocity vector data showing two 3D jet columns in the left atrium.

View the video content online at www.cvcasejournal.com.

magnetic resonance velocity magnitude images demonstrated two widely separated jets at A1-P1 and A3-P3 leaflets, in close agreement with the echocardiograms in the two-chamber (Figure 3C, Video 6) and short-axis (Figure 3D, Video 7) views. Visualization of 3D flow traces provided conclusive evidence for the double jet orifice, as marked by the two high-velocity streams in the left atrium (Figure 6A, Video 8). Direct quantification of mitral flow and aortic flow was performed by tracking the valve movement at each cardiac phase and adjusting the interrogation plane accordingly. Late systolic MR was identified by the delayed onset of mitral reverse flow relative to the aortic forward flow (Figure 6B), and the integration of the reverse flow resulted in Rvol of 24 mL. MR was determined to be mild, as the results were consistent across the two CMR methods and in broad agreement with findings on echocardiography. Volumetric measurements on the basis of MRI are also listed in Table 1.

Because of the reduced ejection fraction, PMVT during exercise, history of syncope, and family history, the patient was referred for heart failure and electrophysiologic evaluation. Genetic testing revealed a variant of uncertain significance (VUS), c.3734T>A (p.Leu1245Gln), in *MYH7*, a gene associated with autosomal-dominant hypertrophic cardiomyopathy (MedGen UID: 501195), dilated cardiomyopathy (MedGen UID: 37831), and LV noncompaction (MedGen UID: 349005) as well as sudden cardiac death in hypertrophic cardiomyopathy.[7] The leucine residue is highly conserved and not present in population databases, which suggests a rare (e.g., private) mutation more likely to be pathogenic. On the basis of the patient's phenotype, PMVT, and this *MYH7* variant, we recommended screening first-degree relatives with echocardiography, Holter monitoring, and cascade genetic testing of this VUS, given that we are highly suspicious that this variant contributes to her phenotype, and we are clinically treating this as a VUS-leaning pathogenic.

The precise electrophysiologic consequences of the patient's situation were unclear, given bileaflet mitral valve prolapse with mitral annular disjunction but only mild to moderate MR and no late gadolinium enhancement or anterior T-wave inversions, markers for high-risk mitral valve prolapse syndrome. Although she had suspected long-QT syndrome, her bursts of PMVT did not occur at times of particularly long QT intervals, suggesting that these were not a forme fruste of torsades de pointes, but rather a non-QT-dependent

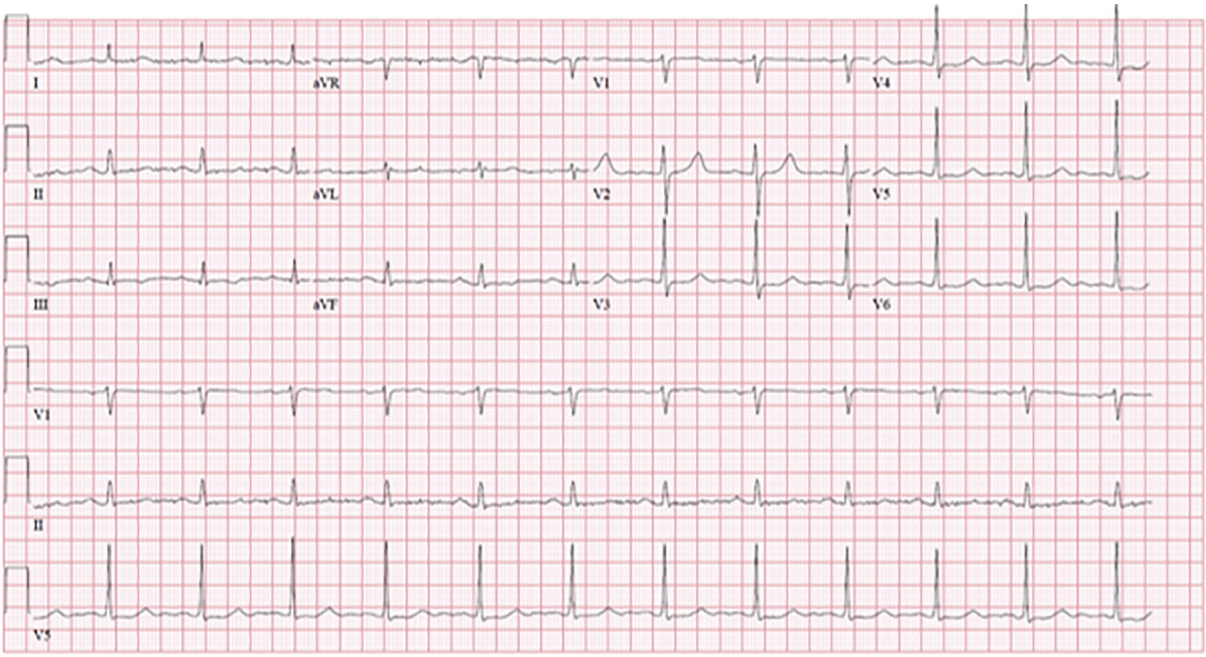

Figure 1 Electrocardiogram demonstrating prolonged QT interval of 452 msec (corrected QT interval 497 msec).

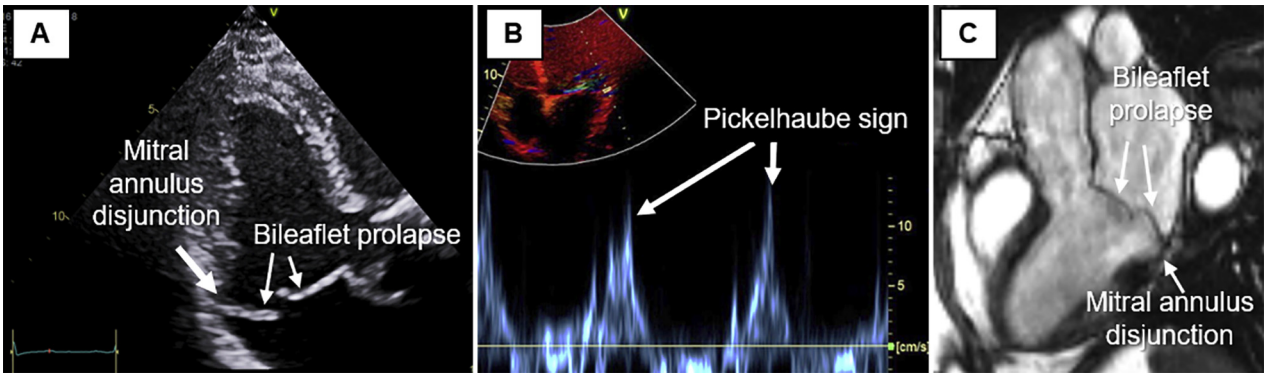

Figure 2 Mitral valve prolapse–related factors detected by echocardiography and magnetic resonance imaging. **(A)** Three-chamber transthoracic echocardiogram with mild mitral annular disjunction. **(B)** Tissue Doppler of the lateral annulus illustrating the Pickelhaube sign (sudden apical myocardial movement in late systole). **(C)** Three-chamber cine MRI also demonstrating the disjunction. All these factors have been associated with arrhythmias in mitral valve prolapse.

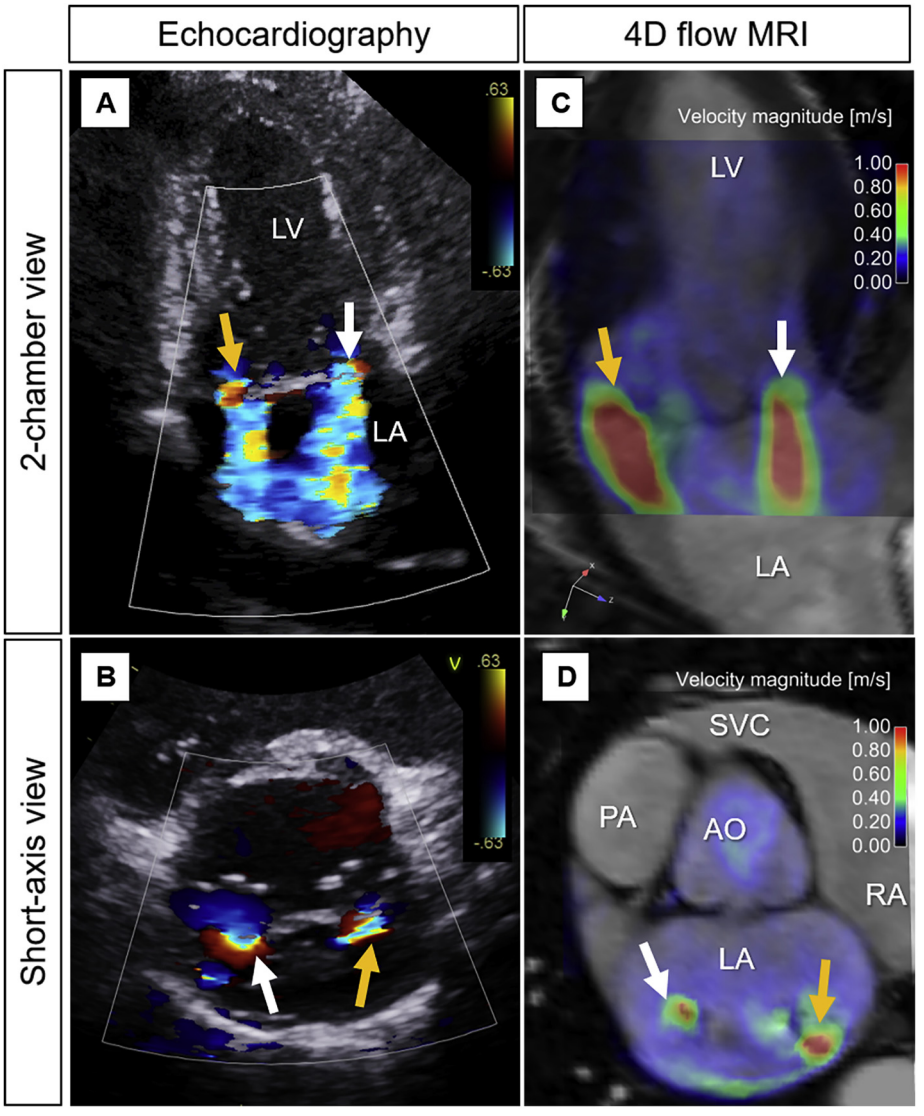

Figure 3 Double-orifice MR captured by color Doppler echocardiography and 4D flow MRI. Velocity magnitude on cross-sectional 4D flow MRI data are shown, where corresponding two-dimensional cine MRI data are shown on the background. **(A, C)** Two centrally directed regurgitant jets (anterior jet, *white arrow*; posterior jet, *orange arrow*) captured in two-chamber view. **(B, D)** Anatomic locations of regurgitation visualized in short-axis view. *AO*, Aorta; *LA*, left atrium; *LV*, left ventricle; *PA*, pulmonary artery; *RA*, right atrium; *SVC*, superior vena cava.

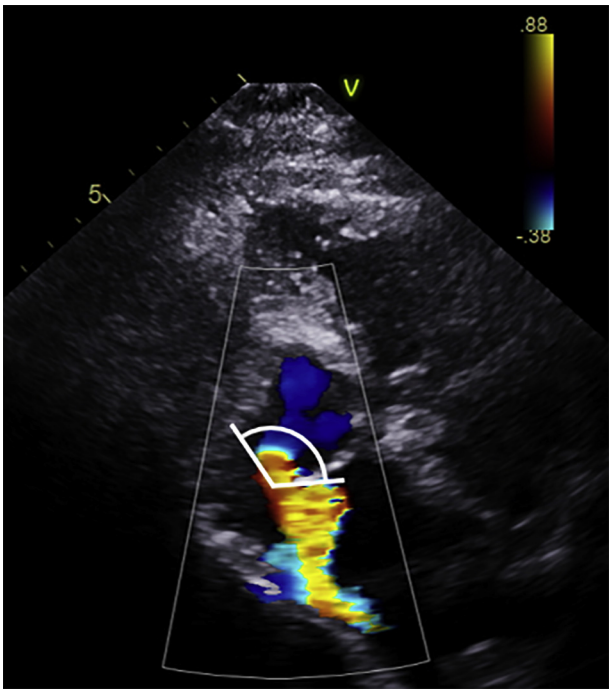

Figure 4 Wall-constrained posterior regurgitation flow convergence zone on color Doppler echocardiography. *White lines* indicate that the observed angle of convergence zone was reduced to 120° from its expected full hemispheric angle of 180°. Thus, the calculated EROA was reduced by one third.

mechanism. Most concerning was her recurrent syncopal episodes with a strong family history of sudden death and a potentially pathogenic mutation in *MYH7*. The patient was recommended to undergo defibrillator implantation for primary prevention. Given her history of sinus bradycardia in the past and the likely need to treat with rate-slowing agents as well as the potential advantage of atrial pacing for long-QT syndrome, a dual-chamber transvenous implantable cardioverter-defibrillator was recommended and implanted.

DISCUSSION

This case illustrates multimodal imaging assessment of challenging MR with multiple orifices and nonholosystolic occurrence. Multiple orifices can exaggerate jet area on color Doppler, and the summation of individual orifice parameters increases the overall error. Nonholosystolic MR causes overestimation in severity when the instantaneous maximum EROA, vena contracta width, and proximal isovelocity surface area radius are considered, while the actual amount of Rvol is reduced. Also, the use of constant EROA ignores the variation that occurs even in the context of late-systolic MR, as shown in a recent study.[8] The volumetric method predicts Rvol indirectly using the difference between LV stroke volume and aortic forward flow volume. This indirect approach can, in theory, overcome the aforementioned limitations, but each component has intrinsic error. When the two components are subtracted, overall uncertainty increases as the individual errors propagate as the root sum of squares, and the subtraction makes it an even larger relative error. This may be one of the reasons for the large discrepancy between the LV volume and the mitral pulsed Doppler approach, which assumes a flat flow profile across the dilated mitral annulus. Given the conflicting regurgitant parameters on echocardiography, further assessment of MR severity was obtained on MRI, which was also needed for assessment of cardiomyopathy.

Four-dimensional flow MRI is an emerging technique that is useful to investigate 3D blood flow behavior in cardiac chambers and great vessels.[6] This case demonstrates how 4D flow MRI can capture MR flow features similar to echocardiography, with additional clarity given to regurgitant jet structure. Furthermore, 4D flow MRI was able to provide direct measurement of Rvol by adjusting the flow quantification plane tracking the valve movement over the cardiac cycle.[9] A recent study of 114 patients with valve diseases showed excellent internal flow consistency across all four valves directly quantified with 4D flow MRI with automated valve tracking (~6-mL difference between LV and RV stroke volumes).[10] Although the accuracy of Rvol by 4D flow MRI against the clinical standard CMR volumetric method needs further investigation, the CMR method also suffers from the propagation of individual measurement errors, as discussed in the previous paragraph.

Four-dimensional flow MRI has a few technical limitations hindering its widespread clinical use. First, a long scan time (~10 min) is needed to acquire data, which makes it sensitive to arrhythmias and body movement. Second, data processing is time consuming, as one needs to deal with a large time-series 3D data set that requires correction and segmentation before analysis. Third, it requires dedicated data analysis software that may not be available at most clinical sites. Finally, the trade-off between spatiotemporal resolution and scan time

Table 1 List of echocardiographic and MRI measurements for MR assessment

	Echocardiography			MRI	
LV end-diastolic volume (mL)	154			166	
LV end-systolic volume (mL)	68			88	
LV stroke volume (mL)	86			78	
LV ejection fraction (%)	56			47	
MR assessment method	**LV volume***	**Mitral PW Doppler†**	**PISA**	**LV volume**	**4D flow MRI**
EROA (cm^2)	0.17	0.5	0.24	NA	NA
MR volume (mL)	21	60	30	20	24
Regurgitant fraction (%)	24	71	35	26	31

NA, Not applicable; *PISA*, proximal isovelocity surface area; *PW*, pulsed-wave.
*Difference of LV and LV outflow tract stroke volumes.
†Difference of mitral annular and LV outflow tract stroke volumes, which is an outlier measurement, likely because of the assumption of a flat flow profile through the enlarged mitral annulus.

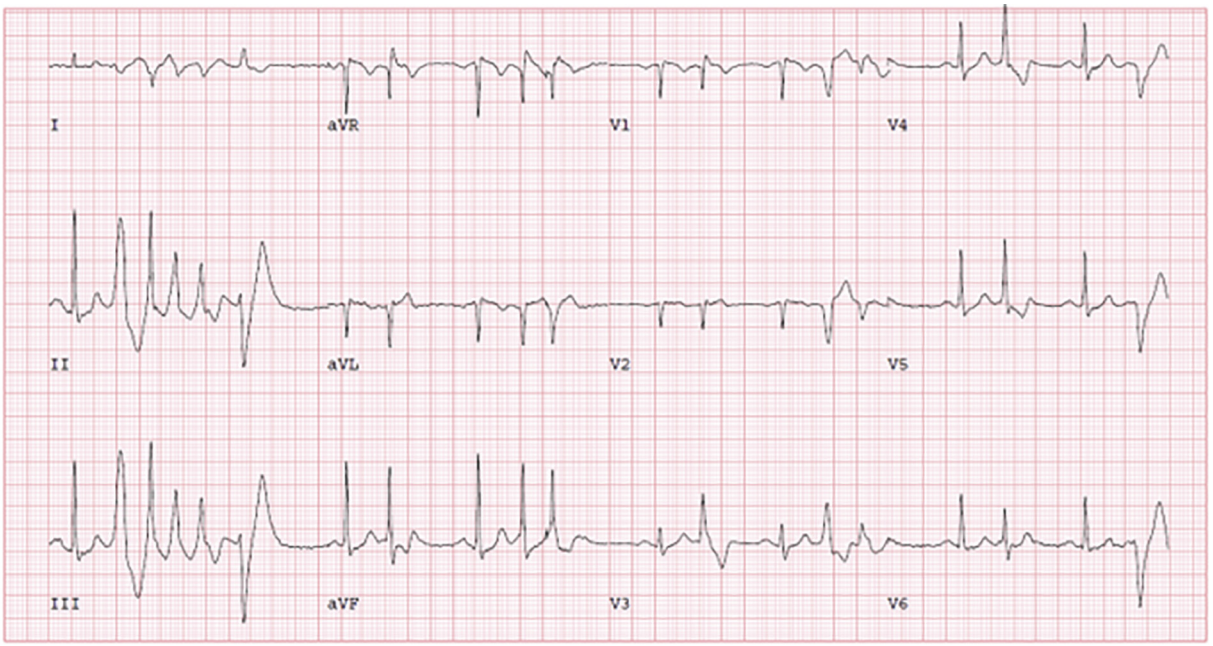

Figure 5 Electrocardiogram during recovery after stress echocardiography demonstrating a five-beat run of rapid PMVT.

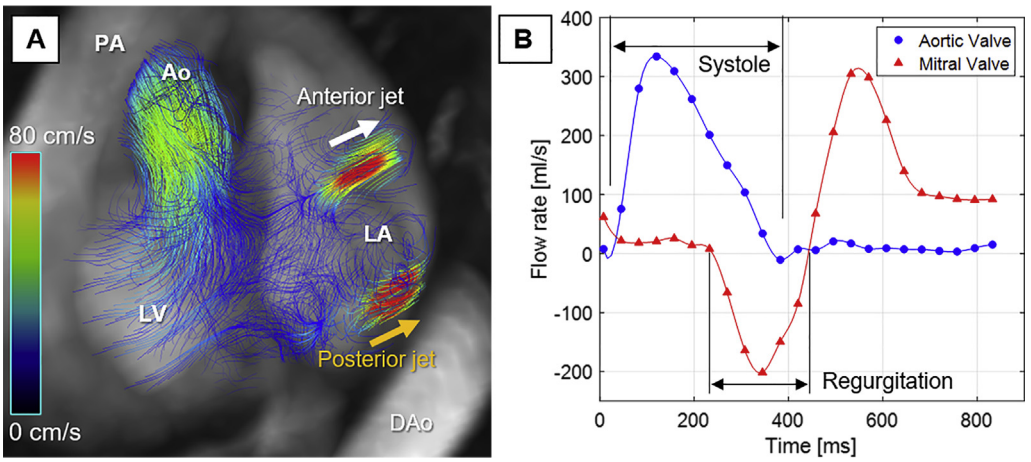

Figure 6 Volumetric visualization of regurgitant jets and flow quantification by 4D flow MRI. **(A)** Three-dimensional streamlines at late systole illustrating two distinct regurgitant jets. **(B)** Transvalvular flow rate profiles for aortic and mitral flow. The profiles were acquired by repositioning measurement planes to the location of valves at each cardiac phase. *Ao*, Aorta; *DAo*, descending aorta; *LA*, left atrium; *LV*, left ventricle; *PA*, pulmonary artery.

limits voxel size to 2 to 3 mm on a side, making the method prone to partial volume effects in regions of high-velocity shear. Efforts are under way to reduce scan time (~2 min)[11] and to use deep learning to streamline data processing.[12] Also, commercial products are now equipped with 4D flow MRI analysis function (e.g., Circle CVI, Pie Medial Imaging, and Arterys), which should extend availability of the technique. However, it remains too early to demonstrate the clinical benefit of adding 4D flow MRI to a clinical MR assessment routine. This case report is meant to illustrate the potential utility of the technique.

As the patient was known to have significant mitral valve prolapse, CMR was performed not only to assess MR but to detect high-risk markers for mitral valve prolapse syndrome to evaluate the need for mitral valve surgery and risk for arrhythmias Although CMR exhibited bileaflet prolapse with mitral annular disjunction and a hypermobile mitral annulus (systolic curling motion[13] or Pickelhaube sign[1,2] on echocardiography), no evidence was found for fibrosis. However, the patient demonstrated very worrisome runs of PMVT in the context of (1) prior syncope with exercise, (2) a strong family history of sudden cardiac death occurring in both parents and a paternal uncle with persistent evidence for mildly reduced ejection fraction, and (3) genetic testing showing a VUS-leaning pathogenic in *MYH7*. She was started on guideline-directed medical therapy but was intolerant of all but a low-dose angiotensin receptor blocker. An implantable cardioverter-defibrillator was inserted with an atrial wire in case future bradycardia (native or medication induced) necessitated pacing and

rate responsiveness. Because her MR was quantified in the mild to moderate range with excellent functional capacity, surgery was deferred with follow-up by serial exercise echocardiography.

CONCLUSION

Our case illustrates the use of multimodal imaging to comprehensively assess a challenging MR case using echocardiography, CMR, and 4D flow MRI. Direct regurgitant flow quantification using 3D flow information from 4D flow MRI may aid in reaching a more direct and definitive assessment of MR severity compatible with clinical symptoms.

SUPPLEMENTARY DATA

Supplementary data related to this article can be found at https://doi.org/10.1016/j.case.2020.08.001.

REFERENCES

1. Ignatowski D, Schweitzer M, Pesek K, Jain R, Muthukumar L, Khandheria BK, et al. Pickelhaube spike, a high-risk marker for bileaflet myxomatous mitral valve prolapse: sonographer's quest for the highest spike. J Am Soc Echocardiogr 2020;33:639-40.
2. Muthukumar L, Rahman F, Jan MF, Shaikh A, Kalvin L, Dhala A, et al. The Pickelhaube sign: novel echocardiographic risk marker for malignant mitral valve prolapse syndrome. JACC Cardiovasc Imaging 2017;10:1078-80.
3. Recusani F, Bargiggia GS, Yoganathan AP, Raisaro A, Valdes-Cruz LM, Sung HW, et al. A new method for quantification of regurgitant flow rate using color Doppler flow imaging of the flow convergence region proximal to a discrete orifice. An in vitro study. Circulation 1991;83:594-604.
4. Zoghbi WA, Adams D, Bonow RO, Enriquez-Sarano M, Foster E, Grayburn PA, et al. Recommendations for noninvasive evaluation of native valvular regurgitation: a report from the American Society of Echocardiography developed in collaboration with the Society for Cardiovascular Magnetic Resonance. J Am Soc Echocardiogr 2017;30:303-71.
5. Pu M, Vandervoort PM, Greenberg NL, Powell KA, Griffin BP, Thomas JD. Impact of wall constraint on velocity distribution in proximal flow convergence zone: implications for color Doppler quantification of mitral regurgitation. J Am Coll Cardiol 1996;27:706-13.
6. Markl M, Schnell S, Wu C, Bollache E, Jarvis K, Barker AJ, et al. Advanced flow MRI: emerging techniques and applications. Clin Radiol 2016;71:779-95.
7. Wilcox JE, Hershberger RE. Genetic cardiomyopathies. Curr Opin Cardiol 2018;33:354-62.
8. Uretsky S, Aldaia L, Marcoff L, Koulogiannis K, Hiramatsu S, Argulian E, et al. The effect of systolic variation of mitral regurgitation on discordance between noninvasive imaging modalities. JACC Cardiovasc Imaging 2019;12:2431-42.
9. Roes SD, Hammer S, van der Geest RJ, Marsan NA, Bax JJ, Lamb HJ, et al. Flow assessment through four heart valves simultaneously using 3-dimensional 3-directional velocity-encoded magnetic resonance imaging with retrospective valve tracking in healthy volunteers and patients with valvular regurgitation. Invest Radiol 2009;44:669-75.
10. Kamphuis VP, Roest AA, Ajmone Marsan N, van den Boogaard PJ, Kroft LJ, Aben J-P, et al. Automated cardiac valve tracking for flow quantification with four-dimensional flow MRI. Radiology 2019;290:70-8.
11. Ma LE, Markl M, Chow K, Huh H, Forman C, Vali A, et al. Aortic 4D flow MRI in 2 minutes using compressed sensing, respiratory controlled adaptive k-space reordering, and inline reconstruction. Magn Reson Med 2019;81:3675-90.
12. Berhane H, Scott M, Elbaz M, Jarvis K, McCarthy P, Carr J, et al. Fully automated 3D aortic segmentation of 4D flow MRI for hemodynamic analysis using deep learning. Magn Reson Med 2020;84:2204-18.
13. Dejgaard LA, Skjølsvik ET, Lie ØH, Ribe M, Stokke MK, Hegbom F, et al. The mitral annulus disjunction arrhythmic syndrome. J Am Coll Cardiol 2018;72:1600-9.